

DETAILED MONITORING AND PRELIMINARY EVALUATION OF A LARGE FAÇADE-MOUNTED PV ARRAY

Anton Driesse
Steve Harrison
Solar Calorimetry Laboratory
Queen's University,
Kingston, Ontario, K7L 3N6, CANADA
e-mail: driessea@post.queensu.ca; harrison@me.queensu.ca

ABSTRACT

A 20 kW grid-connected PV array, one of the larger systems in Canada, was installed on the Queen's University campus in Kingston during the first half of 2003. Planning for the array began more than 18 months earlier with the identification of an appropriate façade having good exposure to both solar radiation and passers-by.

From its inception, the project included continuous performance monitoring as a core objective for both teaching and research purposes. Thus, the level of detail that is captured here far exceeds that which is typically available on such systems. The sensors and apparatus installed for this purpose will be presented, and the software that supports the monitoring will also be briefly introduced.

After several months of nearly continuous operation the data have already shown a number of events and performance characteristics of interest, including automatic inverter shut-downs and the effects of shadows and reflections, to name but two. The latest and most significant observations from the data are reported with pertinent graphs and figures.

1. INTRODUCTION

A new 20 kW grid-connected PV array, facade-mounted or otherwise, is no longer the curiosity it once would have been. Nevertheless as the design work for the system at Queen's University progressed, unexpected issues arose, and significant design changes were required (1). Similarly, detailed monitoring was not anticipated to yield fundamental new insights, yet as data collection progresses we are challenged to find explanations for unexpected observations. This paper presents our recent observations,

some expected and some not, and our attempts to provide plausible, if not definitive explanations.

1.1 System Overview

The most efficient way to describe the array is by photograph. Fig. 1 illustrates the four rows of modules mounted as awnings above the windows of the top four floors of this seven-story building. The module slope and position relative to the windows are a compromise between electrical yield and aesthetics, and also between shading, daylight and view. The balance of system is installed in the adjacent building where the electrical room is more spacious. The specifications of the system are summarized in TABLE 1 below.



Fig. 1: Goodwin Hall, Queen's University at Kingston

The modules are electrically connected as 12 parallel strings of 22 modules each, for a total of 264 modules. The balance of system components are wired in sequence as follows:

1. String current shunts (12)
2. Fuses (12)
3. String combiner
4. DC disconnect
5. Array current shunt
6. Inverter
7. AC meter
8. Isolation transformer
9. AC disconnect
10. Distribution panel

TABLE 1: SYSTEM SPECIFICATIONS

Location	Kingston, Ontario, Canada
Latitude	44° North
Slope	70° from horizontal
Azimuth	5° West of South
Nominal PV Power	19.8 kWp
Modules	Photowatt PW750 75Wp, multi-crystalline
Inverter	Xantrex PV 20208 20kWp, 208 V, 3-phase
Estimated annual yield using RETScreen (2)	20.3 MWh

2. MONITORING EQUIPMENT

The original objectives for monitoring of this system were dominated by the educational component, i.e. to provide an accurate portrait of a typical, operating photovoltaic installation, with data to serve as the basis for learning exercises and projects. The focus on thermal issues during the design phase highlighted the research potential and led to a proliferation of thermocouples on the facade. (See the summary in TABLE 2.) Electrical operating parameters are easier to measure, and their smaller number was expected to capture all the details of interest.

Further details are given in context where needed, but two clarifications are appropriate here. First, the intelligent power meter measures instantaneous voltage and current on the AC side, and then calculates dozens of parameters such as real and reactive power, total harmonic distortion and frequency, as well as keeping track of total energy flow to and from the grid. These parameters are not yet recorded in the database, but will be in the near future.

Second, the inverter maintains an internal log of the key operating parameters as well as operating mode and fault codes. This log is downloaded periodically, and merged with the data from the other sensors. It includes AC power, voltage and current.

TABLE 2: SENSOR SUMMARY

Parameter	Sensor Type	Qty.
Solar radiation	Silicon photodiode pyranometer	4
Module temperature	Copper-constantan thermocouple pad	12
Air temperature	Copper-constantan thermocouple probe (30 cm)	18
String current	10A/50mV shunt	12
Array current	100A/50mV shunt	1
Array voltage	600V/10V isolated transducer	2
Inverter current (AC)	Current transformer	3
Inverter power (AC)	Intelligent power meter	1
Wind speed and direction	Cup anemometer and vane	1
Ambient temperature	Thermistor	1
Humidity	(inactive)	1

2.1 Data Acquisition Hardware

A major requirement of the monitoring system was that data be available in real time via the Internet in order to maximize impact and educating potential. Computer-based data acquisition cards could have provided the network connectivity, but this option was rejected in favour of a system of modules with embedded processors and built-in networking in order to achieve greater reliability and reduced maintenance. It is unclear whether this was achieved, though, since the modules do crash and require resets and software upgrades on occasion – and their “black-box” nature makes them rather difficult to troubleshoot. A useful benefit of real-time operation is that any problems with the system become apparent immediately as they occur.

In terms of performance, the data acquisition modules provide 16-bit resolution combined with a sampling rate of approximately once per second. The resolution is ample for the accuracy limits of the sensors. The sampling rate would seem to be more than adequate as well, but the inverter operation causes frequent perturbations in DC voltage and DC current that are barely captured at this rate. This is further discussed in section 3.4.6.

2.2 Data Archiving Software

The core of the monitoring system is the database that stores the measurements. For this function we have access to an industrial-strength software system that is tailor-made to store time-series data. In fact, a single installation is used for multiple monitoring projects, and the PV system data represents but a small fraction of its content.

The database collects data either through proprietary interface software, or through industry standard protocols such as Modbus and OPC (OLE for Process Control). It also makes data available for analysis through proprietary tools or again through standard protocols such as ODBC (Open Database Connectivity). All of these methods are used.

3. OBSERVATIONS

3.1 Energy

Electricity generation is the fundamental purpose of the system and a performance summary is an appropriate first step. We used the RETScreen photovoltaic model (2) to estimate monthly yield based on a few basic system parameters and these values are shown in the second column of TABLE 3. For comparison with actual data the month of July is split in two to reflect the fact that the system began operating on July 18, 2003. The first row in the table thus represents the last 14 days of the first July, and the last row before the total represents the first 17 days of the next July to make a full year.

TABLE 3: CALCULATED AND MEASURED ENERGY

Month	kWh expect.	kWh logged	Days logged	Days running	kWh adjust.
Jul.	904	748	14	14	748
Aug.	1964	2024	31	31	2024
Sept.	1762	1997	30	30	1997
Oct.	1620	1605	31	31	1605
Nov.	985	1084	30	30	1084
Dec.	940	1321	28	31	1463
Jan.	1543	1712	31	31	1712
Feb.	1719	2172	29	29	2172
Mar.	2029	1428	25	31	1771
Subtotal	13466	14091	249	258	14575
Apr.	1904				
May	1952				
Jun.	1864				
Jul.	1098				
Total	20284				

The column “kWh logged” indicates the energy production calculated from the periodic power readings recorded by the inverter. This number was roughly adjusted to account for several days of incomplete logs. The adjusted production to the end of March appears to be about 8% higher than predicted by RETScreen. This is encouraging, but no major conclusions can be drawn of course, since the expected output represents a long-term average.

The accuracy of the inverter log, power calculation and adjustments were verified by comparing the total energy figure for the period July 18, 2003 to March 29, 2004 to a

manual reading of the external AC power meter at the end of that period. These two figures differ by less than 0,5 %, which gives a level of comfort, albeit not proof, that the above table is valid.

3.2 Solar Radiation

Each level of the array is equipped with a small pyranometer mounted at the extreme eastern edge to measure incident solar radiation in the plane of the array, as illustrated in Fig. 2. The four-fold redundancy invites comparison, and a plot of five-minute averages reveals some interesting discrepancies between winter and summer readings as shown in Fig. 3 and Fig. 4 respectively.



Fig. 2: Pyranometer mounting location.

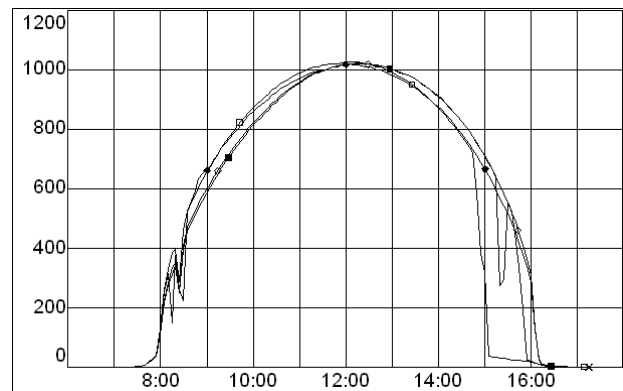


Fig. 3: Solar radiation [W/m^2] on December 13, 2003.

At solar noon in December sunlight arrives very nearly perpendicular to the plane of the array, and for this reason the highest readings are recorded at that time, as expected. The fact that the peaks for the different readings do not occur at the same time, is attributed to differences in mounting angle of the sensors – a difference that is easily seen, but not so easily corrected.

The most curious aspect of these graphs is that the summer graph shows the 7th floor sensor peaking at a significantly

lower value than the other three – 740 W/m² compared to 805 W/m². This was initially attributed to the sensor itself or the shunt resistor for lack of a better explanation, but when the discrepancy gradually disappeared through the fall and into the winter, another explanation was needed.

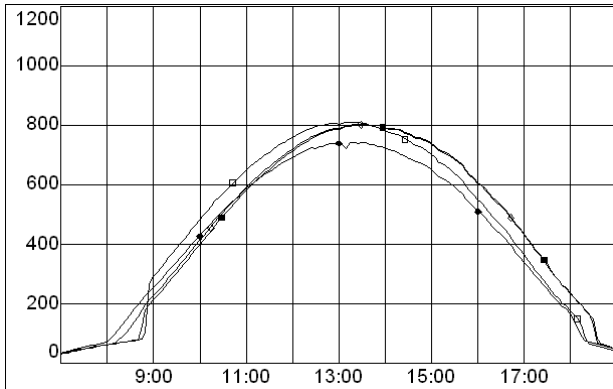


Fig. 4: Solar radiation [W/m²] on August 13, 2003.

The most plausible explanation at this time is that the lower three sensors pick up significant beam radiation reflected by the light concrete immediately above the arrays. The reflection would be partly diffuse, but the high summer sun would certainly produce stronger reflections in the direction of the pyranometer below than would the lower winter sun.

The question that immediately arises is whether the effect of this reflection is also evident as higher string current measurements. The answer is still outstanding, however, since the currents are also affected by several other factors.

3.3 Thermal Profile

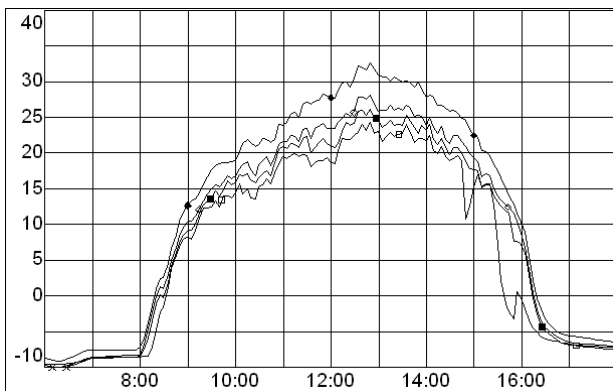


Fig. 5: Module temperatures [C] on each floor Dec. 13, 2003. The values are averages of three sensors mounted on back of a single module at each floor. The upper curve is for the 7th floor; the lower for the 4th floor.

During the design process concern about high temperatures was centred around the possible effects on the building interior and occupants. High temperatures are of course undesirable from a PV performance point of view as well. A portion of the heat rejected by the PV cells is carried away by air rising along the front and rear of the modules, and in this installation the rising hot air causes higher air and cell temperatures on the upper levels. As expected, the cumulative effect is greater at times when there is little wind.

3.4 Electrical Performance

3.4.1 Effects of Temperature

The temperature gradient has a two-fold negative impact on PV electrical performance. The higher temperature on the upper floors reduces the maximum power output of those cells, but it also lowers the voltage at which that maximum output is obtained. All 12 strings in the system are wired in parallel to a single inverter so they are forced to operate at the same voltage; however a single voltage cannot allow maximum power to be extracted from all the modules, therefore the total power is reduced even further.

The inverter is continually adjusting the DC operating voltage in order to extract the maximum power, so it is difficult to evaluate the magnitude of these effects directly. According to the manufacturer’s specifications (see below), a 10 C temperature difference leads to 4.3% less power and a decrease in string voltage of about 17 V.

TABLE 4: PHOTOVOLTAIC ARRAY SPECIFICATIONS

		Cell	Module	String	Array
I_{sc}	A	4.84	4.84	4.84	58.1
V_{oc}	V	0.598	21.5	474	474
I_{mpp}	A	4.42	4.42	4.42	53.0
V_{mpp}	V	0.47	17.0	375	375
P_{mpp}	W	2.09	75.2	1,655	19,863
Cell voltage temperature coef.: (dV/dT) = -2.17 mV/°C.					
Cell current temperature coef: (dI/I)/dT = 0.034%/°C					
Power temperature coefficient: (dP/P)/dT = -0.43%/°C					

A simple 2-cell model can be used to show that cells (and similarly modules or strings) at different temperatures and should operate at an intermediate voltage when connected in parallel to capture the overall maximum power. At this voltage the hotter cells generate slightly less current than their cooler counterparts, and the combined maximum power level is slightly less than the sum of the individual maxima. This is illustrated in Fig. 6 where the voltage scale reflects the number of series cells in a string.

Around the time of the peak insolation and peak current at noon, the array is operating in the range 360-365 V. This is approximately where the simple PV model suggests it

should be, however the measured currents are about 5% lower than the model predicts. With the measured insolation level just over the magic 1000 W/m^2 there are at least other factors that could be contributing to this: wire resistance and cell mismatch.

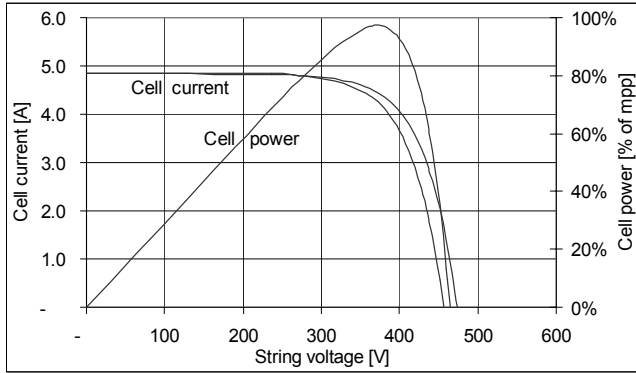


Fig. 6: Simple PV model showing the effect of a 10°C cell temperature difference with solar radiation at 1000 W/m^2 .

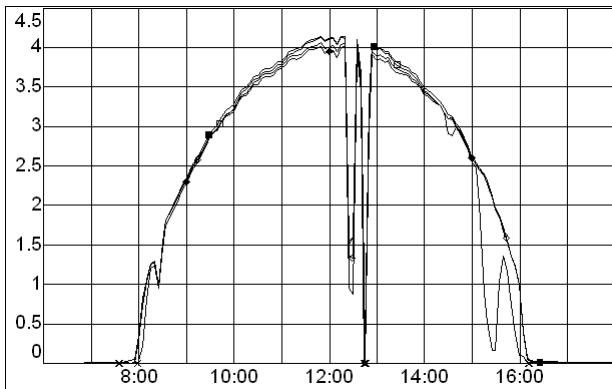


Fig. 7: Current [A] for the middle string on each of the 4 floors. The trace sequence from upper to lower curve is: 5^{th} , 4^{th} , 6^{th} , 7^{th} . (The sudden drops are discussed later.)

3.4.2 Wire Resistance

The combiner box is quite a distance away in the adjacent building, so wiring for each string creates an additional series resistance that shifts the operating point (all else being equal) and reduces the available power. Since the cable lengths are different for each string, this could also cause an operating point mismatch in a similar manner to the temperature differentials.

The total wire length per string ranges from approximately 113 to 178 m. The wire is AWG10 stranded, which has a resistance of about $3.3 \text{ m}\Omega/\text{m}$. At the nominal string current of 4.42 A, the resulting voltage drops would be in the range

of 1.7 to 2.6 V, or 0.4-0.7% of the nominal array voltage. (See the details in TABLE 5.) Thus, the effect of this resistance on the operating point should be minimal, and easily overshadowed by the temperature effects. It is also worth noting that the associated power loss in the wiring would be less than 0.6% at the nominal power output level.

TABLE 5 VOLTAGE DROPS AT NOMINAL CURRENT

		Lateral Position		
		West	Center	East
Floor	7^{th}	2.2	1.9	1.8
	6^{th}	2.4	2.0	1.7
	5^{th}	2.5	2.1	2.1
	4^{th}	2.6	2.3	1.9

3.4.3 Cell and Module Mismatch

Bypass diodes that are installed for each set of 18 cells limit the effect of severe mismatches, faults and partial shading, but smaller performance mismatches have the effect of limiting the total performance of an entire string, and hence an entire array (3). This system has series strings of 792 cells, and it is virtually certain that there are variations in cell characteristics. This is the most plausible explanation for the lower than expected current measurements.

3.4.4 Automatic Shutdowns

The discontinuities in the current readings of Fig. 7 are actually evidence of the inverter shutting down automatically. According to the inverter software alarm log, the voltage on one of the three phases exceeded the programmed threshold, which was set at 220.5 VAC. On this day, the inverter logs indicate the line-to-line voltage holding quite steady around 218 before the shutdown. Since the logs provide only one sample per minute, and 5 consecutive cycles above the threshold level are sufficient to trigger a shutdown, it appears that a brief surge caused the shutdown.

There are several aspects we note here. First, as soon as the inverter shut down, the grid voltage recorded by the inverter dropped by about 5 volts. In other words, the fact that the inverter was feeding 17 kW into the grid caused the voltage at its output terminals to increase by about 2.5%. It seems likely that this is in large part because the inverter must overcome the losses in the isolation transformer. The distribution panels and wiring on the grid side of the transformer have current ratings much higher than the PV output and should not incur voltage drops of this magnitude. If the transformer is indeed responsible for most of this voltage change, then voltage further out on the grid did not really exceed the specified threshold.

Second, with the arrival of the cold, bright days of January, the inverter shut down more and more often, setting a record of 22 times in succession between 10am and 2 pm on January 10th. Each time after shutting down, the inverter sensed that the grid voltage was back to normal (which it was) and started up again. But immediately after starting it would sense a high voltage and shut down again. There appears to be no dead band or hysteresis associated with this threshold to prevent cycling, and only the 6-minute start-up delay prevented it from cycling more frequently.

Discussions with the manufacturer revealed that shutdowns due to high voltage are common with the factory threshold setting, and upon their recommendation the setting was increased to 222.5 V. There have been very few shutdowns since that change.

3.4.5 Observations during Shutdowns

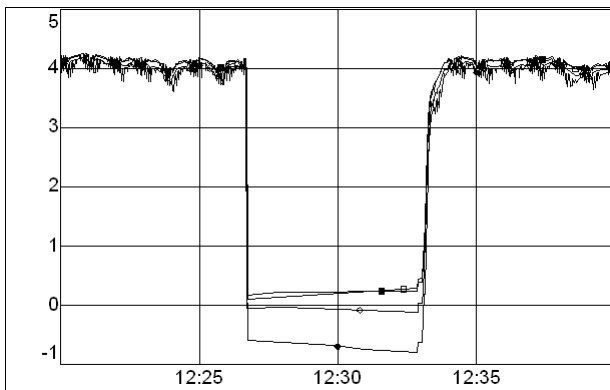


Fig. 8: Currents of the middle strings of each floor during inverter shutdown. The large negative current is on the 7th floor where the cells are hottest.

The frequent shutdowns were disappointing from a performance point of view, but provided some exceptional data as well. As discussed in Section 3.4.1, temperature differences between floors produced small differences in operating point. When the inverter shuts down the total array current drops to zero, and the voltage rises toward V_{oc} . V_{oc} is different for each cell of course, but near V_{oc} the slope of the IV curve is very steep. Thus when the array stabilizes at one voltage, the currents show much more variation as is seen in Fig. 8 below.

3.4.6 High-frequency Signal Components

The time range of the previous figure is sufficiently short that a pattern is discernable in the current variations before and after shutdown. The close-up below confirms this in greater detail. The perturbations in the four currents appear to be somewhat synchronized, and the total current (not shown) shows a similar pattern. Determining the exact

nature of these variations will require further investigation. It seems likely that there is a link with the MPPT (maximum power point tracking) algorithm, which typically fluctuates around the maximum point, but the nature of this link is unclear. Since the sampling rate is around 1 Hz, and there is no filter to prevent aliasing of signals below 60Hz, the actual signal could look quite different.

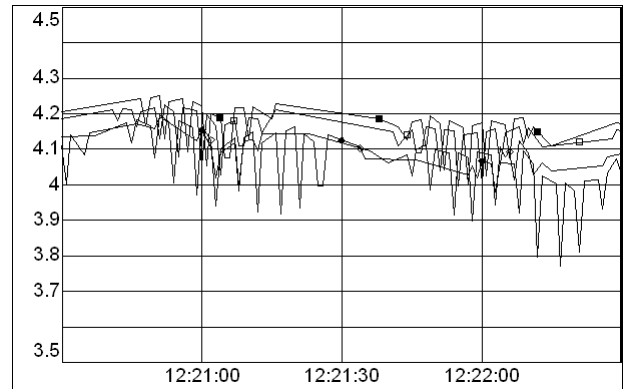


Fig. 9: Close-up of four string currents showing periodic perturbations.

4. CONCLUSIONS

A first examination of data collected on the Queen's University system during 8 months of operation has confirmed the overall operation and permitted insights into a variety of events and phenomena, some of which clearly require and merit further study. Among them are: evaluating the option of using multiple inverters or MPPT units to accommodate the temperature gradient on the facade, and investigating alternate ways of detecting or responding to high grid voltage. Although the data acquisition system has undergone several improvements already since the time it was first installed, further enhancements should be pursued to more accurately capture the details of the DC current and voltage signals.

5. REFERENCES

- (1) Driesse, A., Harrison, S. J. and Lin Q. Analysis and Mitigation of Thermal Effects on a Large Facade-Mounted PV Array, Proceedings of the 2003 ISES Solar World Conference, International Solar Energy Society, 2003
- (2) RETScreen International Photovoltaic Project Model, www.retscreen.net, CANMET Energy Technology Centre, Varennes, 2000
- (3) Wenham, S.R., Green, M.A., and Watt, M.E. Applied Photovoltaics, Centre for Applied Photovoltaics, Australia, 1994.